Analytical investigation of turbulence quantities and cosmic ray mean free paths from 1995-2017

IOP Conf. Series: Journal of Physics: Conf. Series **1100** (2018) 012029 doi:10.1088/1742-6596/1100/1/012029

Analytical investigation of turbulence quantities and cosmic ray mean free paths from 1995-2017

L L Zhao[1], L Adhikari[1], G P Zank[1,2], Q Hu[1,2] and X S Feng[3]

[1] Center for Space Plasma and Aeronomic Research (CSPAR), University of Alabama in Huntsville, Huntsville, AL 35899, USA

[2] Department of Space Science, University of Alabama in Huntsville, Huntsville, AL 35899, USA

[3] State Key Laboratory of Space Weather, National Space Science Center, Chinese Academy of Sciences, Beijing, 100190, People's Republic of China

E-mail: lz0009@uah.edu

Abstract. We use OMNI 1-minute resolution data sets from 1995 through 2017, covering about two consecutive solar cycles, to investigate the solar cycle dependence of various turbulence quantities and cosmic ray (CR) mean free paths. We employ quasi-linear theory (QLT) and nonlinear guiding center theory (NLGC) to evaluate the CR parallel and perpendicular diffusion. We find that in the ecliptic plane at 1 au (1) the fluctuating magnetic energy density $\langle z^{\pm 2} \rangle$, residual energy E_D, and corresponding correlation functions all have an obvious solar cycle dependence. The residual energy E_D is always negative, which indicates that the energy in magnetic fluctuations is larger than the energy in kinetic fluctuations, especially at solar maximum; (2) the correlation length λ for magnetic fluctuations does not show significant solar cycle variation; (3) the temporally varying shear source of turbulence, which is most important in the inner heliosphere, depends on the solar cycle; and (4) high level turbulence will increase CR perpendicular diffusion and decrease CR parallel diffusion, but this trend can be masked if the background interplanetary magnetic field (IMF) changes in concert with turbulence in response to solar activity. These results provide quantitative inputs for both turbulence transport models and CR diffusion coefficient models.

1. Introduction

The transport of cosmic rays (CRs) throughout the heliosphere is determined by the large-scale solar wind (SW) flow and the magnetized turbulence embedded in it. The CR diffusion tensor is the critical factor in simulating the observed temporal and spatial variation in the CR spectra and describes the scattering of CRs by fluctuations in the interplanetary magnetic field (IMF) [1]. Currently, there are several numerical models that couple CR propagation with magnetic turbulence transport and the background IMF evolution [e.g., 2-4]. It is well established that the background IMF periodically changes from solar minimum to maximum ($\sim$ 11 years). However, a detailed understanding of the dependence of turbulence quantities on solar activity, which is another important component of modeling the time-dependent CR modulation, is not yet well understood.

The evolution of low-frequency turbulent fluctuations in the large-scale radially expanding SW plasma can be interpreted in terms of magnetohydrodynamic (MHD) theory [5]. Zank et al. [6] develop a turbulence transport model to describe the evolution of the total energy density in

forward- and backward-propagating modes, the residual energy, the corresponding correlation lengths and the cross-helicity provided the plasma beta is large (> 1). Adhikari et al. [7] study the effect of solar cycle on the evolution of various turbulence quantities based on the Zank et al. [6] model. The SW velocity, source terms, and inner boundary conditions are treated as time dependent. They find that the temporal SW introduces a periodic variability in the magnetic energy fluctuations and correlation length beyond 1 au. Shiota et al. [8] incorporate the Zank et al. [6] model in a three-dimensional (3D) inhomogeneous SW and find reasonable agreement with *Helios* 2 and *Ulysses* measurements. Recently, Zank et al. [9] have derived a coupled 2D and slab turbulence model based on the nearly incompressible (NI) MHD theory, which includes all basic turbulence variables and shows extensive agreement with *Voyager* 2 observations [10]. It is thought that SW fluctuations are highly anisotropic with respect to the direction of the large-scale mean magnetic field. Adhikari et al. [11] investigated anisotropy in magnetic field fluctuations by assuming a 80:20, 70:30, 60:40, and 55:45 initial energy ratio between 2D and slab turbulence at 1 au. They found that the evolving anisotropy ratios in both the energy-containing and inertial range are ordered by the inner boundary ratios, and exhibit similar trends for each initial anisotropy ratio. For slow and intermediate SW in the ecliptic plane at 1 au as used in our study, 2D turbulence dominants (50% - 85%) in the inertial range [12, 13]. Since the 2D and slab energy ratio 80:20 is usually used in theoretical work based on the assumption of a plasma beta ~ 1 or $\ll 1$ in SW or solar corona [e.g., 14-17], we employ an 80:20 energy ratio between 2D and slab turbulence at 1 au. For the correlation scale variability in the SW fluctuation, Weygand et al. [18] suggest that the ratio of slab to 2D correlation scales is 2.55 ± 0.76 (with 0.76 the uncertainty) for the slow SW, 2.15 ± 0.18 for the intermediate SW, and 0.71 ± 0.29 in the fast stream. Following prior studies [e.g., 19-21], we assume the ratio of slab to 2D correlation as 2.0.

Once the turbulence model is determined, the CR diffusion coefficients can be derived from an appropriate energetic particle diffusion theory. Zhao et al. [22] present a detailed analysis of the radial and rigidity dependence of the CR diffusion tensor using the Zank et al. [9] two-component turbulence model. Here, we continue to use quasi-linear theory (QLT, [1]) and nonlinear guiding center (NLGC, [23]) theory, respectively, to evaluate the CR parallel mean free path (MFP) and perpendicular MFP at 1 au. More sophisticated CR diffusion theories have since been developed [e.g., 24-26], but QLT and NLGC provide simple reasonably tractable expressions that have been employed in many energetic particle transport studies. For our purpose, they are sufficiently accurate.

The organization of this paper is as follows: Section 2 presents the data analysis method we employed. Section 3 presents the temporal evolution of various turbulence quantities from 1995 to 2017. Section 4 illustrates the effect of solar activity on CR mean free paths. The last section provides a summary and conclusions.

2. Data Analysis Process

In this paper, we analyze *OMNI* 1-minute resolution data for the magnetic and bulk velocity fields, from 1995 to 2017, covering about two solar cycles. We first calculate the total fluctuation energy density in forward- and backward-propagating modes, the residual energy, and the corresponding correlation functions at 1 au in view of an Elssässer description. Based on these turbulence variables, we further obtain the total fluctuating magnetic field variance and the correlation length as defined in Zank et al. [6, 9], which are essential factors of CR diffusion coefficients calculation.

The method to find the above-mentioned turbulence quantities is similar to that of Zank et al. [27]. The various quantities are calculated for the inwardly and outwardly directed magnetic field separately, because the orientation of the IMF determines whether a mode is forward or backward propagating. The process of calculating various turbulence quantities is as follows: 2

hr interval data containing the X, Y, and Z components of the magnetic field and SW velocity, the proton density, and temperature are taken. The missing data within an interval are discarded, then we check whether the following criteria are satisfied: (i) the mean square fluctuations of the magnetic and bulk velocity field should be smaller than the square of the corresponding mean fields, and (ii) the intervals should contain at least N/2 good data points (N is the total number of data points in one interval). Criterion (i) is used for all three components of magnetic and velocity fields, since it excludes intervals with irregular magnetic and velocity fluctuations. Various features of the SW plasma are speed related. For example, Dasso et al. [12] found that the anisotropy of SW fluctuations differs in fast and slow SW. Since more than 92% of the SW velocity is less than 450 kms^{-1} after classification by criteria (i) and (ii) in our study, we do not consider SW speed bins here. The next step is to find the direction of the background IMF in each retained interval, which is neither along the radial nor the azimuthal direction in the ecliptic plane at 1 au. Here, we employ the minimum variance analysis (MVA) technique to determine the unit vector of the background IMF in each interval from the measured magnetic field vector data. The detailed theory and derivation of the MVA technique can be found in Sonnerup and Scheible [28]. The variance ellipsoid [28, 29], given by MVA technique, defines the variance along an arbitrary chosen direction in the GSE coordinate system. The vector with the smallest variance is close to the local mean field direction, and assumed to be the direction of the background IMF in each interval. Since we consider transverse fluctuations, the observed magnetic field and velocity field components in each interval are projected into the two directions that are perpendicular to the minimum variance direction. The following calculation is carried out in these two directions respectively. We first introduce the definition of the Elsässer variables:

$$\mathbf{z}^{\pm} = \mathbf{u} \pm \frac{\mathbf{b}}{\sqrt{\mu_0 \rho}}, \tag{1}$$

where μ_0 is the magnetic permeability, ρ is the mass density, $\mathbf{u}$ is the fluctuating velocity field, and $\mathbf{b}$ is the fluctuating magnetic field. The Elsässer variables $\mathbf{z}^+$ ($\mathbf{z}^-$) represent the forward (backward) propagating modes with respect to the IMF orientation. We further introduce the following moments of the Elsässer variables $\mathbf{z}^{\pm}$ and the lagged variables $\mathbf{z}^{\pm'}$ [6, 9]:

$$\langle z^{+2} \rangle \equiv \langle \mathbf{z}^+ \cdot \mathbf{z}^+ \rangle = \langle u^2 \rangle + \langle b^2/\mu_0\rho \rangle + 2\langle \mathbf{u} \cdot \mathbf{b}/\sqrt{\mu_0\rho} \rangle; \tag{2}$$

$$\langle z^{-2} \rangle \equiv \langle \mathbf{z}^- \cdot \mathbf{z}^- \rangle = \langle u^2 \rangle + \langle b^2/\mu_0\rho \rangle - 2\langle \mathbf{u} \cdot \mathbf{b}/\sqrt{\mu_0\rho} \rangle; \tag{3}$$

$$E_D \equiv \langle \mathbf{z}^+ \cdot \mathbf{z}^- \rangle = \langle u^2 \rangle - \langle b^2/\mu_0\rho \rangle; \tag{4}$$

$$L^+ \equiv \int \langle \mathbf{z}^+ \cdot \mathbf{z}^{+'} \rangle dr \equiv \langle \mathbf{z}^+ \cdot \mathbf{z}^+ \rangle \lambda^+ = \lambda^+ \langle z^{+2} \rangle; \tag{5}$$

$$L^- \equiv \int \langle \mathbf{z}^- \cdot \mathbf{z}^{-'} \rangle dr \equiv \langle \mathbf{z}^- \cdot \mathbf{z}^- \rangle \lambda^- = \lambda^- \langle z^{-2} \rangle; \tag{6}$$

$$L_D \equiv \int \langle \mathbf{z}^+ \cdot \mathbf{z}^{-'} + \mathbf{z}^{+'} \cdot \mathbf{z}^- \rangle dr \equiv \lambda_D E_D. \tag{7}$$

Here, $\langle z^{+2} \rangle$ and $\langle z^{-2} \rangle$ respectively represent the energy density in forward and backward propagating modes, E_D is the residual energy, L^+, L^- and L_D are the corresponding correlation functions, and λ^+, λ^- and λ_D are the corresponding correlation lengths.

According to CR diffusion theory, we need to calculate the 2D and slab turbulence magnetic energies as input for the CR diffusion coefficients. Here we first calculate the total fluctuating magnetic energy $\langle b^2 \rangle$ and correlation length λ using

$$\langle b^2 \rangle = \frac{\langle z^{+2} \rangle + \langle z^{-2} \rangle - 2E_D}{4} \mu_0 \rho; \tag{8}$$

$$\lambda = \frac{L^+ + L^- - L_D}{\langle z^{+2} \rangle + \langle z^{-2} \rangle - 2E_D}. \tag{9}$$

Then we assume that the total energy in fluctuations can be divided into majority 2D and minority slab energies with a fixed ratio 80:20, and the slab correlation length λ_s is assumed to be twice the 2D correlation scale λ_{2D}, thus $\lambda_s = 2\lambda_{2D} = 2\lambda$.

3. Results

3.1. Solar cycle dependence of turbulence quantities

Figures 1 and 2 show the temporal evolution of the energy density in forward- and backward-propagating modes $\langle z^{\pm 2} \rangle$ and the corresponding correlation functions $L^{\pm}$, the residual energy E_D, and the corresponding correlation functions L_D. Figure 1 shows the data sets for two solar cycles for the outwardly directed IMF, and Figure 2 is for the inwardly directed IMF. All of these turbulence quantities are derived from Equations (2)-(7). From Figure 1 and 2, we can see that all turbulence quantities vary with solar activity and show solar cycle dependence. It is

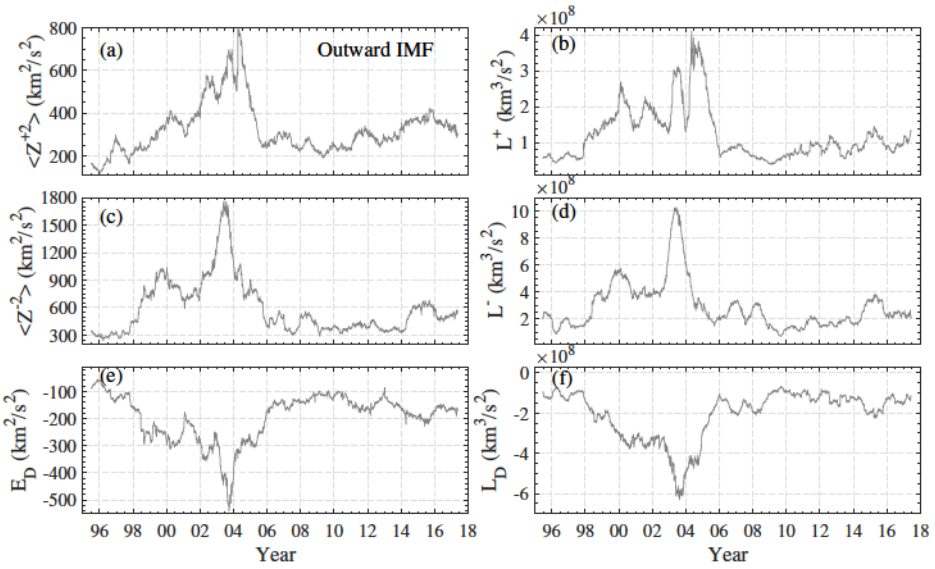

Figure 1. The temporal evolution of (a) the energy density in forward propagating modes $\langle z^{+2} \rangle$ and (b) the corresponding correlation function L^+; (c) the energy density in backward propagating modes $\langle z^{-2} \rangle$ and (d) the corresponding correlation function L^-; and (e) the residual energy E_D and (f) the corresponding correlation function L_D for the outwardly directed IMF.

interesting to notice that the values of the residual energy E_D and the corresponding correlation function L_D are always negative, which illustrates that the energy in magnetic fluctuations is larger than the energy in kinetic fluctuations, especially at solar maximum. The energy densities $\langle z^{\pm 2} \rangle$, residual energy $|E_D|$, and the associated correlation functions $L^{\pm}$ and $|L_D|$ are all positively correlated with solar cycle. For example, the energy density in forward-propagating mode is about 1500 $km^2 s^{-2}$ during solar maximum while it is about 360 $km^2 s^{-2}$ during solar minimum. The corresponding correlation function is about $9.0 \times 10^8 km^3 s^{-2}$ for solar maximum and is about $1.2 \times 10^8 km^3 s^{-2}$ during solar minimum. When calculating correlation functions in Equation (5)-(7), we assume the maximum time lag t is 1 hour. Most previous studies use the spatial lag r, where the auto-correlation function of the Elsässer variable becomes $1/e$ of the maximum values, to determine the correlation length. Since the auto-correlation function

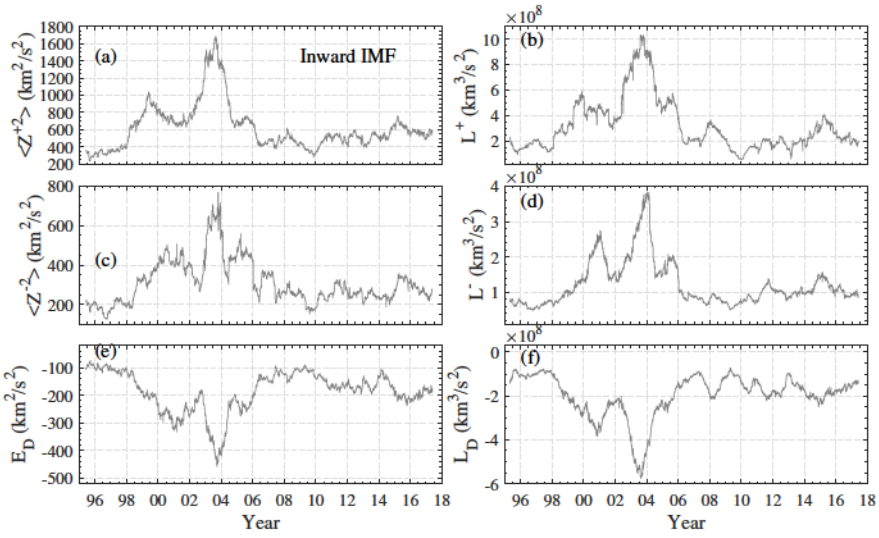

Figure 2. Same as Figure 1, but now for the inwardly directed IMF.

of Elsässer variable drops rapidly, a spatial lag at $1/e$ of the maximum value is closer to zero lag. Therefore, limiting our analysis to a specified maximum time lag seems reasonable.

Figure 3 depicts the influence of solar activity on a critical term in the shear source expression

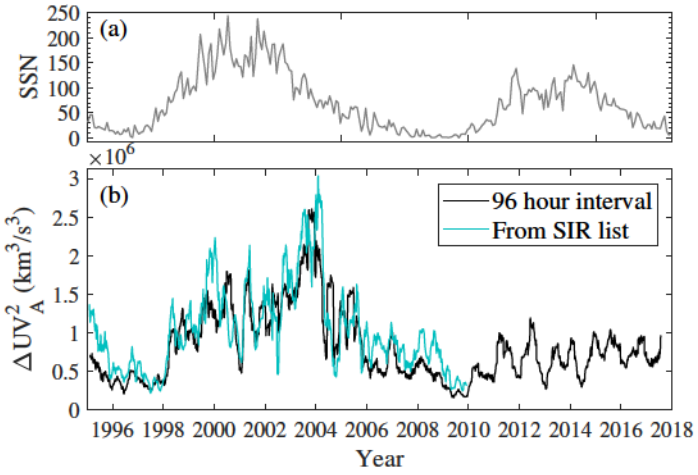

Figure 3. The top panel (a) shows the monthly averaged sunsport number (SSN). Panel (b) shows the temporal evolution of the critical term ΔUV_A^2 for the shear source. The black line represents the result calculated in each 96 hour interval. The green line represents the result calculated in the time interval determined by start time and end time of each shear interaction region (SIR) event during for 1995-2009.

plotted as a reference. The complete form of shear source terms that we consider is given by Zank et al. [9] as

$$S_{\langle z^{\pm 2}\rangle} = C_{sh}^{\pm}\frac{r_0|\Delta U|V_A^2}{r^2}; \qquad S_{E_D} = C_{sh}^{E_D}\frac{r_0|\Delta U|V_A^2}{r^2}, \tag{10}$$

where the parameters $C_{sh}^{\pm}$ and $C_{sh}^{E_D}$ are parameterized strengths of the shear source of energy in forward and backward modes and the residual energy, respectively. $C_{sh}^{+} \neq C_{sh}^{-} \geq 0$, and $C_{sh}^{E_D}$ can be 0, positive, or negative. r_0 is a reference location. ΔU is the difference between fast and slow SW speeds, and V_A is the background Alfv́en speed. In Figure 3, we calculate the product $\Delta U V_A^2$ in each 96 hr interval to include the structure of streams. The green line is calculated in the time interval determined by start time and end time of each stream interaction region (SIR) event during 1995-2009, which were compiled by Jian et al. [30, 31]. Our result agrees well with the SIR list for 1995-2009, and shows a rather clear solar cycle dependence, which indicates that the shear source term of turbulence is also correlated with solar activity.

Figure 4 shows the monthly averaged 2D and slab turbulence magnetic energies and the corresponding correlation lengths respectively calculated from Equation 8 and 9. The red dashed lines are for inwardly directed IMF, and the blue lines are for outwardly directed IMF. We can see that there is little difference between inward and outward IMF modes. We have assumed $\langle b_{2D}^2 \rangle : \langle b_s^2 \rangle = 80\% : 20\%$ and $\lambda_s = 2\lambda_{2D} = 2\lambda$. We can see a clear solar cycle dependence in the turbulence energy. Solar maximum carries more turbulent energy than solar minimum, which is caused by the frequent generation of shocks that generate turbulence [27]. In contrast, the correlation lengths show no discernible solar cycle variation. Wicks et al. [32] studied the spatial correlation properties of solar wind using *ACE* and *Wind* measurements, and found that the correlation length for components of the magnetic field does not show an obvious solar cycle dependence, which is consistent with our results. From Figure 4, we notice that the slab turbulence energy $\langle b_s^2 \rangle$ in year 2003 is four times larger than that in year 2009, and the correlation length λ_s in 2003 is two times larger than in 2009. The averaged value of λ_s is

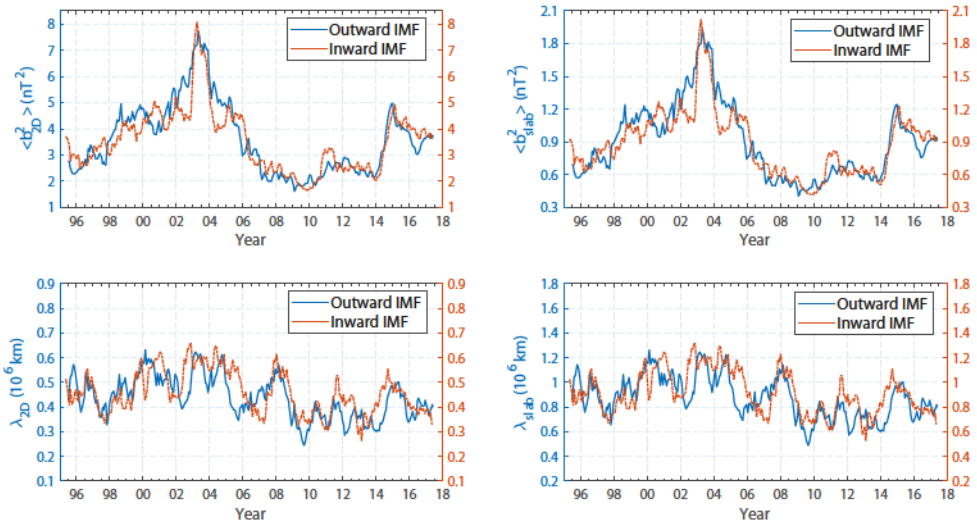

Figure 4. The temporal evolution of monthly averaged 2D turbulence magnetic energy $\langle b_{2D}^2 \rangle$ (left top) and the corresponding correlation length λ_{2D} (left bottom), slab turbulence magnetic energy $\langle b_s^2 \rangle$ (right top) and the corresponding correlation length λ_s (right bottom). A ratio of 2D and slab energy of 80:20 and $\lambda_s = 2\lambda_{2D} = 2\lambda$ has been assumed.

about 0.88×10^6 km. This value is a little smaller than previous studies of correlation lengths for magnetic field fluctuations in the solar wind. For example, Tu and Marsch [33] gave a value of the correlation length for the Elsässer variables as $\lambda \approx 265 R_E \approx 1.7 \times 10^6$ km using single-spacecraft measurements. Matthaeus et al. [34] investigated the value of λ using multiple-spacecraft measurements, and suggested a value of $\lambda \approx 1.3 \times 10^6$ km. However, these previous results didn't consider the effect of solar activity. One can get larger correlation lengths by

increasing the length of interval. Shiota et al. [8] also have analyzed extensively the effect on correlation lengths when using longer intervals. They found that a longer interval data set may not be helpful in determining correlations within the inertial range of SW turbulence. This is because a longer interval may introduce some structures associated with large scale flows into the analysis, which then leads to an increase in the correlation functions and correlation lengths. For our analysis, 2 hours is the most suitable length of interval that yields reasonable correlation lengths when compared with *Voyager* 2 observations [10].

3.2. The effects of solar activity on CR diffusion

Figures 5 shows the effects of solar activity on CR parallel $\lambda_{\parallel}$ (blue line), perpendicular $\lambda_{\perp}$ (red line), and radial mean free path λ_{rr} (grey line) for a proton with rigidity 445 MV (corresponding to a 100 MeV proton) for the outward IMF mode. As described in Zank et al. [19], the parallel mean free path (mfp) based on standard QLT and assuming magnetostatic turbulence is approximated by

$$\lambda_{\parallel} = 6.2742 \frac{B_0^{5/3}}{\langle b_s^2 \rangle} \left(\frac{P}{c}\right)^{1/3} \lambda_s^{2/3} \left[1 + \frac{7A/9}{(q+1/3)(q+7/3)}\right], \tag{11}$$

where $q = \frac{5s^2/3}{1+s^2-(1+s^2)^{1/6}}$, $A = (1+s^2)^{5/6} - 1$, and $s = 0.746834 R_L/\lambda_s$. R_L is the particle Larmor radius; P is the particle rigidity; B_0 is the mean magnetic field strength. The analytic form of the perpendicular mfp based on NLGC theory is given by Shalchi et al. [25]

$$\lambda_{\perp} = \left[\sqrt{3}\pi a^2 C \frac{\langle b_{2D}^2 \rangle}{B_0^2} \lambda_{2D}\right]^{2/3} \lambda_{\parallel}^{1/3}, \tag{12}$$

where $a^2 = 1/3$ is a factor related to the gyrocenter velocity. $C = \frac{\Gamma(\nu)}{2\sqrt{\pi}\Gamma(\nu-1/2)}$ is a constant such that $\nu = 5/6$ yields a Kolmogorov [36] spectrum. Note that Equation 12 was derived under the assumption of a specific form of 2D wave spectrum, which is a constant at large turbulence scales. It means that the 2D turbulence spectrum is independent of wavenumber in the energy range in Equation 12.

The radial mfp, λ_{rr}, can be expressed as a function of the heliospheric magnetic field winding angle ψ,

$$\lambda_{rr} = \lambda_{\parallel} \cos^2\psi + \lambda_{\perp} \sin^2\psi, \tag{13}$$

where $\tan\psi = \frac{B_Y}{B_X}$, and B_X (B_Y) is the averaged X (Y) component of the magnetic field in each interval. The winding angle is not therefore a constant in our calculation, but varies with time. In Figure 5, we employ the monthly averaged 2D and slab turbulence energy and corresponding correlation lengths shown in Figure 4 to calculate CR mfps in the ecliptic plane at 1 au. In this figure, we use a mean value of $B_0 = 5.5$ nT at 1 au to focus on the effects of the small-scale turbulence quantities on CR diffusion coefficients. From Figure 5, we can clearly see the solar cycle dependence of $\lambda_{\parallel}$, $\lambda_{\perp}$, and λ_{rr}. The parallel mfp $\lambda_{\parallel}$ during solar maximum (i.e., 2003) is lower than that during solar minimum (i.e., 2009). In contrast, the perpendicular mfp $\lambda_{\perp}$ in the solar maximum is higher than that in the solar minimum. $\lambda_{\parallel}$ is nearly three orders of magnitude larger than the perpendicular mfp $\lambda_{\perp}$ at 1 au. The radial mfp λ_{rr} is dominated by parallel diffusion $\lambda_{\parallel}$ in the inner heliosphere [22], and also has a positive correlation with solar activity. Chhiber et al. [21] studied the effect of solar activity on CR parallel and perpendicular diffusion by varying the turbulence energy amplitude only (normal, half, and double turbulence energy) at the inner boundary, and found that increasing the turbulence magnitude leads to a decrease in parallel mfp and an increase in perpendicular mfp, which is in agreement with Figure 5 where we assumed a fixed value of B_0.

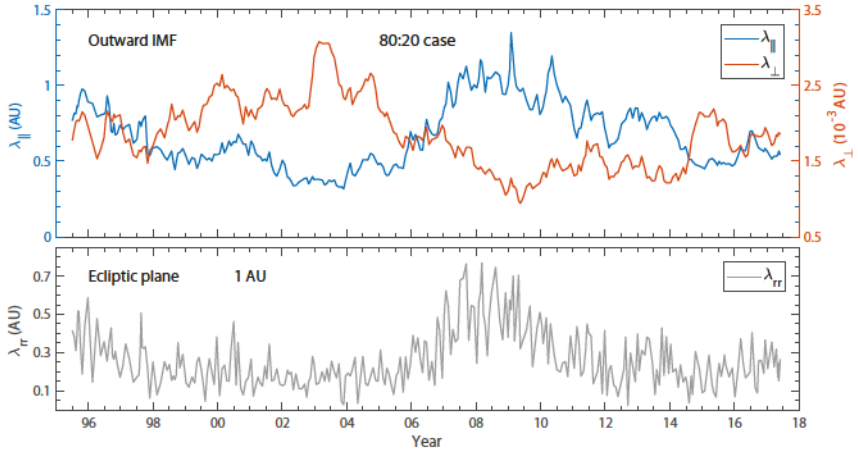

Figure 5. The temporal evolution of CR parallel $\lambda_{\parallel}$ (blue line), perpendicular $\lambda_{\perp}$ (red line), and radial λ_{rr} (grey line) mean free paths for a proton with rigidity 445 MV (corresponding to a 100 MeV proton) in the ecliptic plane at 1 au for outwardly directed IMF. For this example, we have assumed that the background IMF magnitude is constant, $B_0 = 5.5$ nT.

In Figure 6, we use the solar cycle dependent background IMF magnitude obtained from *OMNI* observations to calculate the parallel $\lambda_{\parallel}$ (blue lines), perpendicular $\lambda_{\perp}$ (red lines), and radial λ_{rr} (cyan lines) mfps for the outwardly directed IMF. 2D and slab fluctuation magnetic energies and the corresponding correlation lengths are the same as in Figure 5. By considering the variation of both turbulence quantities and the background IMF magnitude, we find that the solar cycle dependence of CR mean free paths is reduced, since the background IMF magnitude B_0 and turbulence energy $\langle b_s^2 \rangle$ (or $\langle b_{2D}^2 \rangle$) each have the opposite effect on $\lambda_{\parallel}$ (or $\lambda_{\perp}$), as shown by Equation 11 and 12. For example, for a fixed value of background IMF, an increase in $\langle b_s^2 \rangle$ leads to a decrease in $\lambda_{\parallel}$ as shown in Figure 5, while for a fixed $\langle b_s^2 \rangle$, an increase in B_0 leads to an increase in $\lambda_{\parallel}$. Therefore, when we take into account both effects, the solar cycle dependence of $\lambda_{\parallel}$ is somewhat masked but still identifiable. There is an anti-correlation between the parallel mfp $\lambda_{\parallel}$ and perpendicular mfp $\lambda_{\perp}$. In this figure, the averaged value of $\lambda_{\parallel}$ is about 0.9 AU, and the averaged value of $\lambda_{\perp}$ is about 1.6×10^{-3} AU.

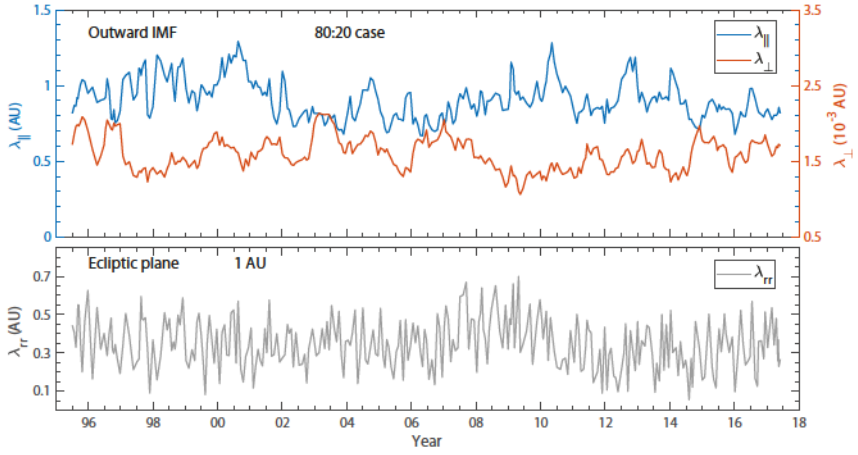

Figure 6. The same as Figure 5, but now for solar cycle dependent background IMF magnitude obtained from the observation.

4. Summary

In this article, we present a detailed analysis of various turbulence quantities and CR mean free paths from 1995-2017 to investigate the effects of solar cycle. Compared to previous empirical time-dependent solutions [7], we use *OMNI* 1-minute resolution data over the last two solar cycles to study the temporal evolution of various turbulence quantities at 1 au for inward and outward IMF modes respectively. The fluctuating magnetic energy densities $\langle z^{\pm 2}\rangle$ and the residual energy E_D all exhibit an obvious solar cycle dependence. This is consistent with previous studies [37, 38] that show a solar cycle dependence for magnetic energy density fluctuations within the inertial range, using *Wind* and *ACE* measurements. The value of $\langle z^{+2}\rangle$ for the inward IMF mode is approximately equal to $\langle z^{-2}\rangle$ for the outward IMF mode, and vice versa, which can be explained from their definitions (Equation 2 and 3). The residual energy E_D, which represents the energy difference between velocity fluctuations and magnetic field fluctuations (Equation 4), is always negative for both inward IMF and outward IMF modes. This illustrates that the energy in magnetic fluctuations is larger than the energy in kinetic fluctuations, especially at solar maximum (Figures 1(e) and 2(e)).

We introduce the correlation function L^+, L^-, and L_D for the Elsässer variables $\mathbf{z}^{\pm}$ and the lagged variables $\mathbf{z}^{\pm'}$ to calculate the correlation length λ of magnetic field fluctuations through Equation 9. We find that the correlation functions evolve similarly to the corresponding energy densities $\langle z^{\pm 2}\rangle$ or the residual energy E_D, and are also correlated with solar cycle. It indicates that the correlation length λ for magnetic fluctuations may not be sensitive to solar cycle. As shown in Figure 4, the correlation length for slab turbulence λ_s (assuming $\lambda_s = 2\lambda_{2D} = 2\lambda$), of which the averaged value is about 0.88×10^6 km, does not show significant solar cycle variation. One can increase the value of the correlation length by using a longer interval length, but it may introduce some structures associated with large-scale flows [8]. Magnetic turbulence energy in 2D $\langle b_{2D}^2\rangle$ and slab $\langle b_s^2\rangle$ fluctuations is positively correlated with solar cycle. The magnetic turbulence energy $\langle b^2\rangle$ in year 2003 (solar maximum) is almost 4 times larger than in 2009 (solar minimum), and also 1.5 times larger than in 2015 (weak solar maximum). There is little difference between inward and outward IMF modes in the evolution of these turbulence quantities, which illustrates that the small-scale SW fluctuations may not depend on the direction of the background magnetic field. Finally, the temporally varying shear source of turbulence, which is most important in the inner heliosphere, also depends on solar cycle.

The above solar cycle dependent turbulence quantities at 1 au can be used as input for both turbulence transport models, which in turn describe the radial evolution of such quantities, and CR diffusion coefficient models. To investigate the solar cycle variation of CR parallel and perpendicular diffusion, one should consider the variation of both turbulence quantities and background large-scale IMF magnitude. We employ quasi-linear theory and nonlinear guiding center theory to model the CR parallel mean free path (mfp) $\lambda_\parallel$ and the perpendicular mfp $\lambda_\perp$, respectively. The temporal evolution of $\lambda_\parallel$, $\lambda_\perp$ and λ_{rr} in the ecliptic plane at 1 au over the recent two solar cycles is calculated. The parallel mfp $\lambda_\parallel$ is about three orders of magnitude larger than the perpendicular mfp $\lambda_\perp$, and dominates the radial mfp λ_{rr} in the inner heliosphere. When we use a fixed value of the IMF, the CR mfps all have a clear solar cycle dependence. The parallel mfp $\lambda_\parallel$ and radial mfp λ_{rr} are anti-correlated with solar cycle while the perpendicular mfp $\lambda_\perp$ is positively correlated with solar cycle. This illustrates that high levels of solar wind fluctuations will increase CR perpendicular diffusion and decrease parallel diffusion if the background IMF strength remains unchanged. However, if the background IMF changes in concert with turbulence levels in response to solar activity, this trend can be masked.

In this study, we present the effect of solar activity on various turbulence quantities and the related cosmic ray diffusion coefficients by analyzing magnetic field and bulk velocity field observed by *OMNI* from 1995-2017. These results provide quantitative input for both cosmic ray propagation models and turbulence transport models, and also provide useful insight for

time-dependent turbulence modeling to understand the long-term cosmic ray modulation which requires turbulence quantities over at least one solar cycle. The solar cycle influence on the global properties of turbulence beyond 1 au still needs further investigation.

Acknowledgments

We acknowledge the partial support of the NSF EPSCoR RII-Track-1 Cooperative Agreement OIA-1655280, NSF-DOE award 1707247, NASA grants NNX08AJ33G, Subaward 37102-2, NNX14AC08G, NNX14AJ53G, A99132BT, RR185-447/4944336 and NNX12AB30G. G.P.Z. is partly supported by the International Space Science Institute (ISSI), both through the award of the 2017 Johannes Geiss Fellowship and in the framework of an International Team Project 504 entitled "Current Sheets, Turbulence, Structures and Particle Acceleration in the Heliosphere". Q.H. acknowledge partial support from SAO subcontract SV4-84017 and NASA grant NNX17AB85G.

References

[1] Jokipii J R 1966 *ApJ* **146** 480
[2] Florinski V, Zank G P and Pogorelov N V 2003 *J. Geophys. Res.* **108** 1228
[3] Engelbrecht N E and Burger R A 2013 *ApJ* **772** 46
[4] Guo X and Florinski V 2016 *ApJ* **826** 65
[5] Zhou Y and Matthaeus W H 1990 *J. Geophys. Res.* **95** 10291
[6] Zank G P, Dosch A, Hunana P, Florinski V, Matthaeus W H and Webb G M 2012 *ApJ* **745** 35
[7] Adhikari L, Zank G P, Hu Q and Dosch A 2014 *ApJ* **793** 52
[8] Shiota D, Zank G P, Adhikari L, Hunana P, Telloni D and Bruno R 2017 *ApJ* **837** 75
[9] Zank G P, Adhikari L, Hunana P, Shiota D, Bruno R and Telloni D 2017 *ApJ* **835** 147
[10] Adhikari L, Zank G P, Hunana P, Shiota D, Bruno R, Hu Q and Telloni D 2017 *ApJ* **841** 85
[11] Adhikari L, Zank G P, Telloni D, Hunana P, Bruno R and Shiota D 2017 *ApJ* **851** 117
[12] Dasso S, Milano L J, Matthaeus W H and Smith C W 2005 *ApJL* **635** L181
[13] Oughton S, Matthaeus W H, Wan M and Osman K T 2015 *Phil. Trans. R. Soc. A* **373** 20410152
[14] Zank G P and Matthaeus W H 1992 *J. Geophys. Res.* **97** 17189
[15] Bieber J W, Matthaeus W H, Shalchi A and Qin G 2004 *GeoRL* **31** L10805
[16] Hunana P and Zank G P 2010 *ApJ* **718** 148
[17] Zank G P, Adhikari L, Hunana P, Tiwari S K, Moore R, Shiota D, Bruno R and Telloni D 2018 *ApJ* **854** 32
[18] Weygand J M, Matthaeus W H, Dasso S and Kivelson M G 2011 *J. Geophys. Res.* **116** A08102
[19] Zank G P, Matthaeus W H and Bieber J W 1998 *J. Geophys. Res.* **103** 2085
[20] Pei C, Bieber J W, Breech B, Burger R A, Clem J and Matthaeus W H 2010 *J. Geophys. Res.* **115** A03103
[21] Chhiber R, Subedi P, Usmanov A V, Matthaeus W H, Ruffolo D, Goldstein M L and Parashar T N 2017 *ApJ* **230** 21
[22] Zhao L L, Adhikari L, Zank G P, Hu Q and Feng X S 2017 *ApJ* **849** 88
[23] Matthaeus W H, Qin G, Bieber J W and Zank G P 2003 *ApJL* **590** L53
[24] Shalchi A 2005 *Physics of Plasmas* **12** 052324
[25] Shalchi A, Li G and Zank G P 2010 *Astrophysics and Space Science* **325** 99
[26] Ruffolo D, Painpanit T, Matthaeus W H and Chuychai P 2012 *ApJ* **747** L34
[27] Zank G P, Matthaeus W H and Smith C W 1996 *J. Geophys. Res.* **101** 17093
[28] Sonnerup B U Ö and Scheible M 1998 *ISSI Scientific Reports Series* **1** 185
[29] Zhao L L, Adhikari L, Zank G P, Hu Q and Feng X S 2018 *ApJ* **856** 94
[30] Jian L, Russell C T, Luhmann J G and Skoug R M 2006 *Solar Physics* **239** 337
[31] Jian L, Russell C T and Luhmann J G 2011 *Solar Physics* **274** 321
[32] Wicks R T, Chapman S C and Dendy R O 2009 *ApJ*, 690, 734
[33] Tu C Y and Marsch E 1995 *Space Science Reviews* **73** 1
[34] Matthaeus W H, Dasso S, Weygand J M, Milano L J, Smith C W and Kivelson M G 2005 *Physical Review Letters* **95** 231101
[35] Shalchi A, Li G and Zank G P 2010 *Astrophysics and Space Science* **325** 99
[36] Kolmogorov A 1941 *Akademiia Nauk SSSR Doklady* **30** 301
[37] Kiyani K, Chapman S C, Hnat B and Nicol R M 2007 *Physical Review Letters* **98** 211101
[38] Hnat B, Chapman S C, Kiyani K, Rowlands G and Watkins N W 2007 *Geophysical Research Letters* **34** L15108